Expression and upregulation of cathepsin S and other early molecules required for antigen presentation in activated hepatic stellate cells upon IFN-γ treatment

Gunter Maubach *, Michelle Chin Chia Lim, Saravana Kumar, Lang Zhuo

Institute of Bioengineering and Nanotechnology, 31 Biopolis Way, The Nanos, #04-01, 138669, Singapore

Abstract

Hepatic stellate cells (HSCs) have been shown to be able to activate T-cells and upregulate expression of surface molecules essential for this process, when treated with IFN-γ. But little is known about the early molecules expressed by activated hepatic stellate cells under the same treatment. In this study, we investigate the effect of IFN-γ on the transcription and expression of these early molecules in hepatic stellate cells. We show on the molecular level that activated rat hepatic stellate cells express the class II transactivator, the invariant chain (CD74), the MHC class II molecules, as well as cathepsin S, all of which are known to be responsible for the initial steps of successful antigen presentation. The mRNA and the protein expression level of these molecules is upregulated by IFN-γ. Importantly, IFN-γ increases cathepsin S activity, suggesting a possible involvement of this protease in CD74 processing. Our data also show that not only can the HSCs take up antigenic proteins, they can also process them. Our comparative study indicates that the rat HSC-T6 cell line displays sufficient similarity to the activated rat HSCs in order to serve as a model for *in vitro* studies on the molecular mechanisms of inflammatory response.
© 2006 Elsevier B.V. All rights reserved.

1. Introduction

Hepatic stellate cells (HSCs), representing 5–8% of the total liver cells, are found in the space of Disse of adult livers between hepatocytes and liver sinusoidal endothelial cells. The classical functions of HSCs are fat storage, vitamin A uptake and metabolism. During the past decades, many authors have shown that HSCs play an important role in defending liver from injuries and at the same time are mediators of hepatic fibrosis by producing profibrotic cytokines and extracellular matrix proteins [1–3]. These different functions of hepatic stellate cells are tightly linked to their transition from a quiescent to an activated phenotype. Recent papers showed the antigen presentation capability of the HSCs

[4,5]. This finding is important as most cell types of the liver contribute to the immune response of the liver in different ways. Hepatocytes produce acute phase proteins [6,7] and liver sinusoidal endothelial cells induce tolerance [8]. The Kupffer cells, resident macrophages of the liver, and resident dendritic cells are known professional antigen-presenting cells [9–13]. The studies from Viñas et al. [4] and Yu et al. [5] described the presence of surface molecules (HLA-DR) and co-molecules (CD40, CD80, CD86), which are necessary for antigen presentation to the T-cells, on the HSCs. In particular, these surface molecules and co-molecules are upregulated when the HSCs are treated with IFN-γ. It was further demonstrated that the HSCs were capable of inducing T-cell proliferation, although less efficiently when compared to the professional antigen presenting cells (APCs), such as Kupffer or dendritic cells, of the liver.

Antigen presentation via MHC class II is a complex process. The early stage of this process involves the induction of the class II transactivator (CIITA), which is the 'master regulator' of the MHC class II expression. CIITA is known to respond to different proinflammatory stimuli and to induce the expression

---

Table 1
RT-PCR primer

Primer	Annealing (°C)	Sequence	Length (bp)
sCathepsin S	55	5′-ACCGAGAATATGAATCATGGTG-3′	127
asCathepsin S		5′-TTCTCGCCATCCGAATATATCC-3′	
sCD74	59	5′-TGGACCCGTGAACTACCCACAGC-3′	234
asCD74		5′-ATATCCTGCTTGGTCACTCC-3′	
sRT1-Bα	55	5′-TCGCCCTGACCACCATGCTCAGCC-3′	187
asRT1-Bα		5′-TCGGGGATCCTCCAGATGGT-3′	
sRT1-Dα	55	5′-TCCCCTCCAGCGGTCAATGTC-3′	259
asRT1-Dα		5′-ACCCGAGAACACACAGGACATTC-3′	
sCIITA type I	55	5′-ACCATTGTGCCCTGCTTC-3′	243
sCIITA type III	52.4	5′-ATCACTCCTCTCTTTACATCATGC-3′	130
sCIITA type IV	55	5′-TAGCGGCAGGGAGACTAC-3′	141
asCIITA type I, III, IV		5′-GGTCAGCATCACTGTTAAGGA-3′	
sβ-actin	55	5′-TTCTACAATGAGCTGCGTGTGG-3	332
asβ-actin		5′-AAGCTGTAGCCACGCTCGG-3′	
sCathepsin L	55	5′-CACCAGTGGAAGTCCACA-3′	122
asCathepsin L		5′-TTCCCGTTGCTGTACTCCCC-3′	

of the classical MHC class II molecules (RT1-B, RT1-D) as well as the accessory molecule invariant chain (CD74, also known as li-chain) (for review see [14]). After the induction, the assembly of class II molecules (RT1-Bα and β, RT1-Dα and β) with the CD74, a type II membrane protein, occurs followed by the step-wise processing of the CD74 into the CLIP (class II associated li-peptide) starting from the C-terminus. The invariant chain directs the MHC class II complex to the late endocytic compartment and prevents the premature loading of the antigen-binding groove. There are many different proteases involved in the processing of CD74. The most effective proteases involved in the last step of this process are cathepsins S and L. These enzymes release the CLIP from the lip10 (leupeptin induced polypeptide). Depending on the cell type, cathepsin L and cathepsin S are involved in this step-wise degradation of the invariant chain in thymic epithelial cells [15] and in B-cells, macrophages and dendritic cells [16–18] respectively.
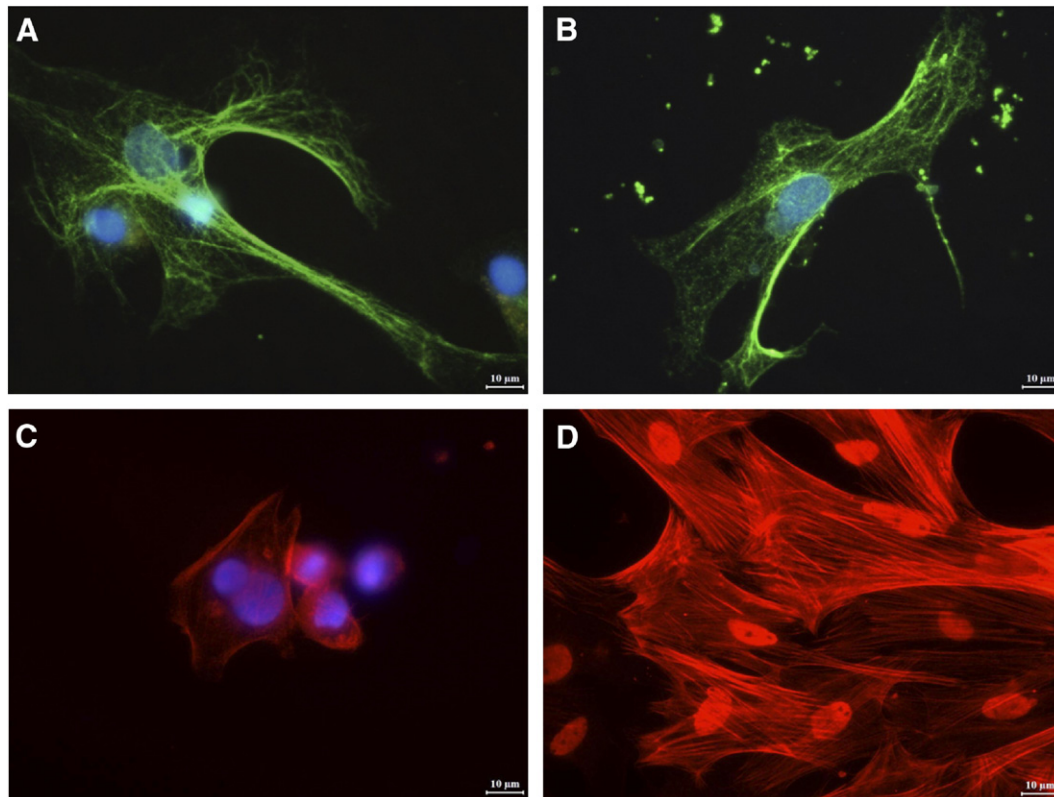

Fig. 1. Identification of primary rat hepatic stellate cells stained with HSC markers. Cells isolated from Wistar rats were labeled after 3 days of cultivation on glass cover slips with (A) GFAP (green); (B) Desmin (green); (C) SMAA (red). (D) The SMAA staining (red) at day ten after isolation showed prominent fiber-like features. (A) to (C) were counterstained with DAPI (blue). Scale bar=10 μm.

Liver fibrosis is a common outcome of chronic hepatic inflammation and the role of hepatic stellate cells in fibrosis is undoubted. In order to search for new targets for a successful treatment, we address the questions: Are these early molecules of antigen presentation and specifically cathepsin S expressed in hepatic stellate cells and are they responsive to the proinflammatory cytokine, IFN-γ. If so, we hypothesize that cathepsin S could be involved in the degradation of the invariant chain in activated hepatic stellate cells. We were also curious to know whether there is any differential expression of these molecules depending on the activation history of HSCs. In case of differentially expressed molecules, they could become a new target for antifibrotic treatment.

2. Materials and methods

2.1. Isolation of primary HSCs

The primary HSCs were isolated from Wistar rats according to a previously published protocol [19]. Briefly, the supernatant was centrifuged at $50 \times g$ for 5 min for several rounds until no visible pellet was observed. The next centrifugation step at $200 \times g$ for 10 min yielded a pellet containing the HSCs.

This pellet was washed once in culture medium and recovered by centrifugation. The cells were re-suspended in culture medium and seeded into 75 cm² culture flasks. For immunocytochemistry, some cells were plated onto glass cover slips in a 24-well culture plate.

2.2. Cell culture

The rat HSC cell line HSC-T6 [20] was a gift from Dr. Scott Friedman (Mount Sinai School of Medicine in New York). The cell line CFSC-3H was kindly provided by Dr. Marcus Rojkind at Albert Einstein College of Medicine, Bronx, New York. The HSC cell lines and the primary rat HSCs were routinely cultured in DMEM (Dulbecco's Modified Eagle Medium), supplemented with 10% FBS and 100 U penicillin/100 μg/ml streptomycin at 37 °C in a humidified atmosphere of 5% CO_2. The HSC cell lines were split twice a week in a 1:3 ratio by trypsinization (0.05% trypsin/0.53 mM EDTA). The primary cells were passaged when required. The primary cells used in all experiments are cell culture activated. All the cell culture media and reagents were purchased from Invitrogen (CA, USA).

2.3. IFN-γ treatment and RNA isolation

HSC-T6, CFSC-3H and activated HSCs were plated into 75 cm² culture flasks and grown overnight at conditions described above. The cells at a confluence of 60–70% were incubated with 10 ng/ml final concentration (equivalent to 100 U/ml) of recombinant rat IFN-γ for 2, 4, 8 and 24 h. The
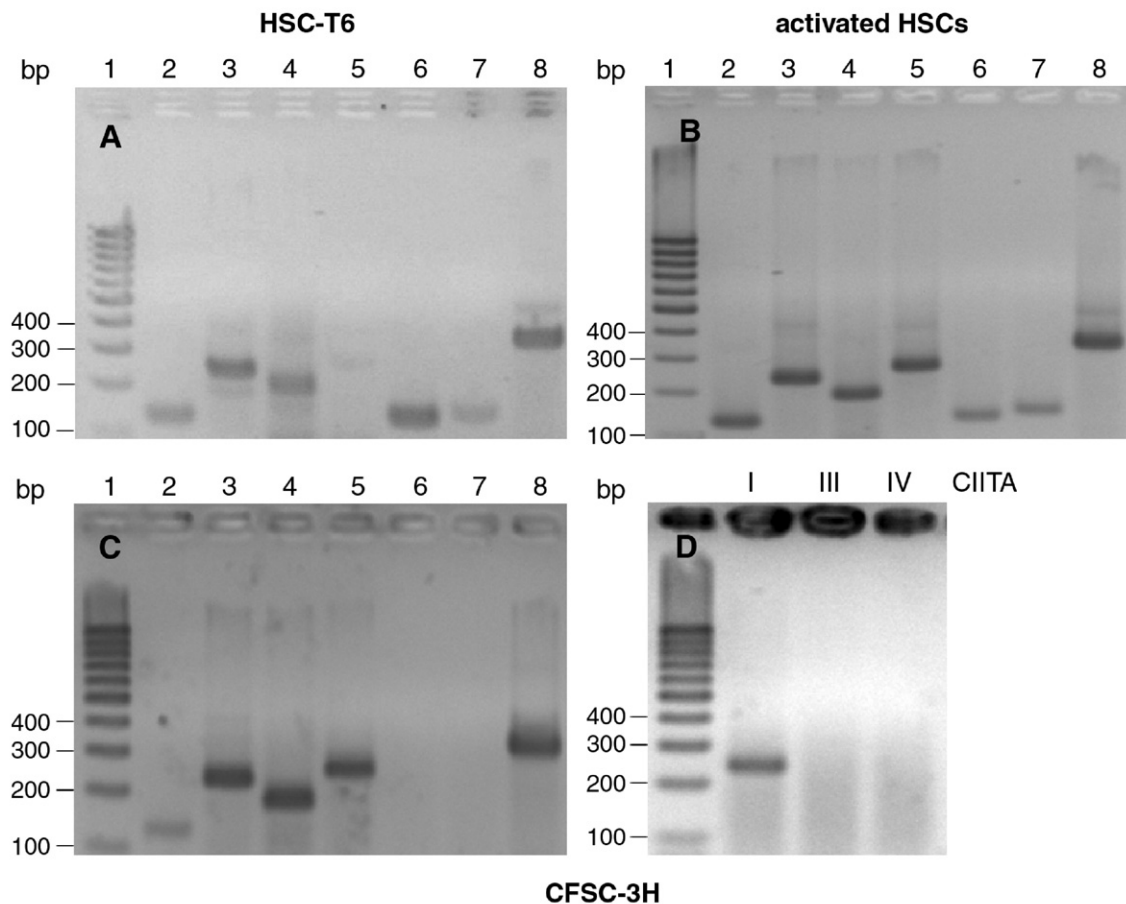

Fig. 2. OneStep RT-PCR analysis of key molecules involved in the early steps of antigen presentation. Total RNA extracted from the HSC-T6 cell line (A), primary HSCs cultured for 36 days (B) and CFSC-3H (C) was analyzed by RT-PCR using primers indicated in Table 1. Lane 1: 100 bp MW ladder (bp), 2: cathepsin S, 3: invariant chain (CD74), 4: RT1-Bα, 5: RT1-Dα, 6: CIITA type IV, 7: CIITA type III, and 8: β-actin. All products detected had the expected size and were confirmed by sequencing. Because we did not detect the mRNA for CIITA types III and IV in CFSC-3H, a RT-PCR for CIITA type I was performed (D). This demonstrates that important molecules involved in the early stage of antigen presentation are expressed in HSCs.
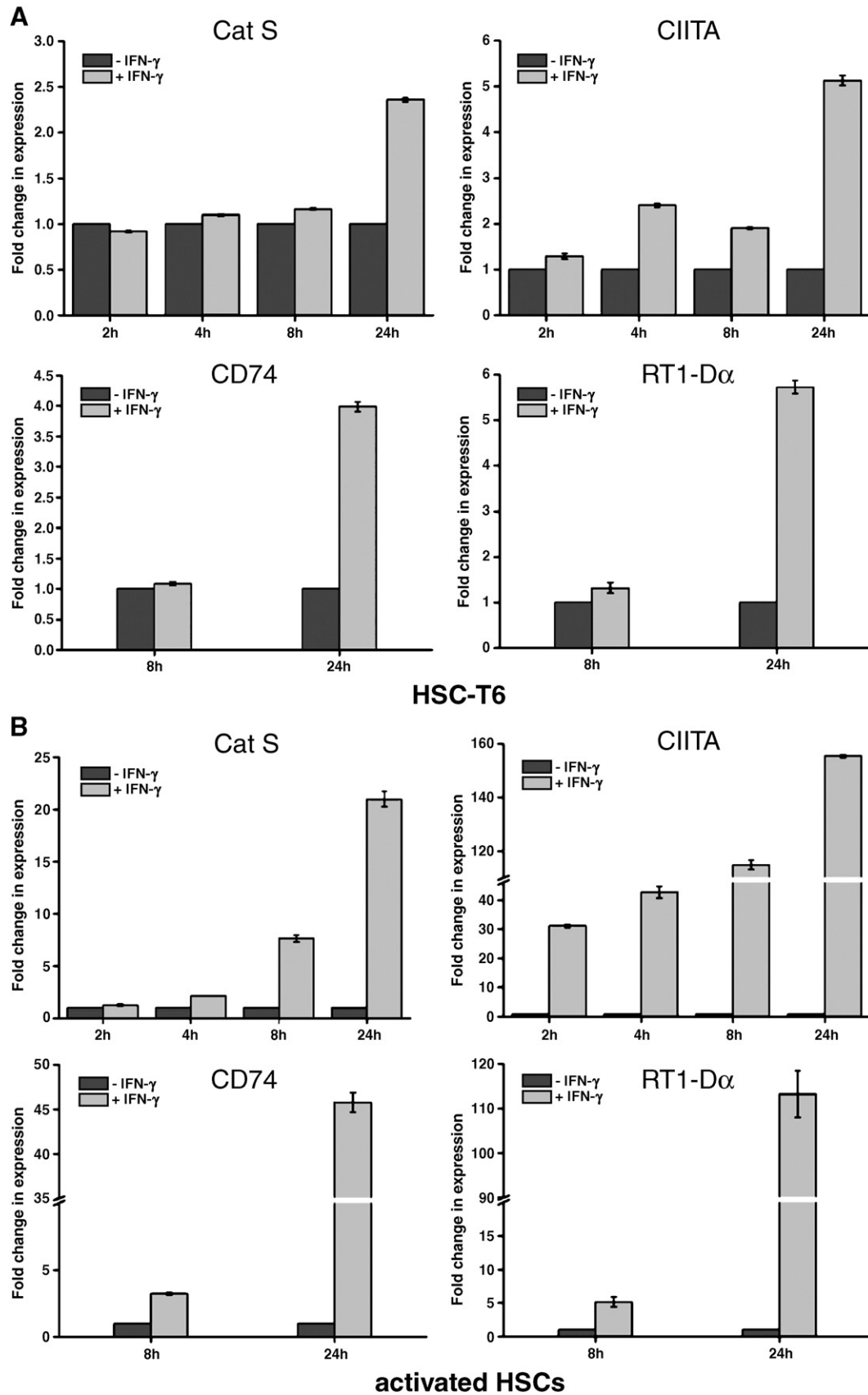
Fig. 3. (A–C) Quantitative analysis of the change in cathepsin S, CIITA, CD74 and RT1-Dα transcript level upon treatment with IFN-γ using real-time RT-PCR. After treatment with IFN-γ for 2, 4, 8 and 24 h, total RNA was extracted from the three different HSCs (activated HSC, HSC-T6 and CFSC-3H). The RNA was reverse transcribed and real-time RT-PCR was performed. The results were expressed as fold change in gene expression compared to the untreated samples using the relative quantification method for HSC-T6 (A), activated HSCs (B) and CFSC-3H (C). The upregulation of all transcripts by IFN-γ is demonstrated for all studied HSCs.
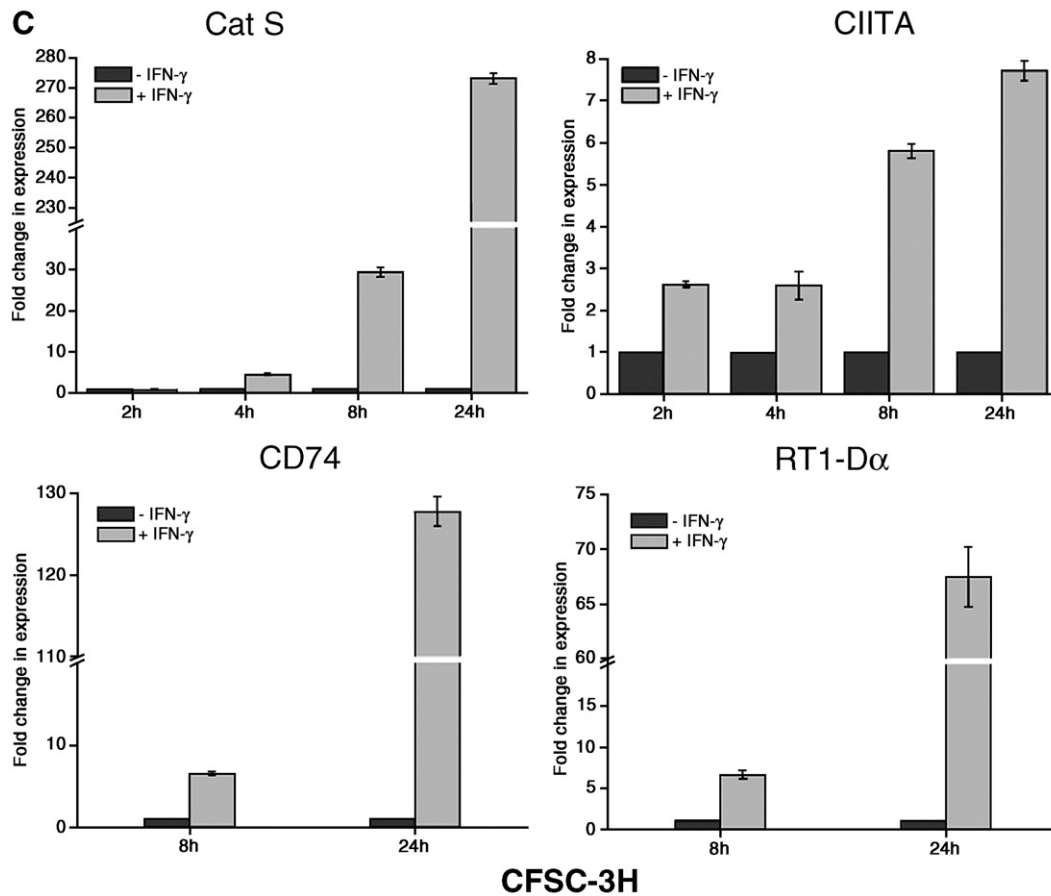
Fig. 3 (*continued*)

recombinant rat interferon-γ (IFN-γ) was purchased from BioVision (CA, USA). Total RNA was isolated using the NucleoSpin RNAII isolation kit (Macherey & Nagel, Germany) according to the manufacturer's protocol. The RNA concentration was measured with the ND-100 spectrophotometer (NanoDrop Technologies, DE, USA).

2.4. OneStep RT-PCR

RT-PCR was performed with the OneStep RT-PCR kit from Qiagen (Germany). 100 ng to 1 μg of total RNA was used in each RT-PCR reaction, depending on the abundance of the transcript. Table 1 shows the information of the primers used. The primer concentration used was 0.6 μM as recommended by the manufacturer. The Q-solution was included in all RT-PCR reactions to minimize nonspecific products. The RT step was carried out for 30 min at 42 °C and followed by deactivation for 15 min at 95 °C. Conditions for PCR were as follow: 10 s for denaturation at 94 °C, 10 s for annealing at an appropriate temperature, and 19 s for synthesis at 72 °C. A total of 40 cycles were performed. We used the PTC-200 thermal cycler (MJ Research, FL, USA). The products were analyzed by electrophoresis in a 3% agarose gel and visualized with ethidium bromide staining. A 100 bp DNA ladder (SM0242, Fermentas, Lithuania) was used as a size marker in all gels. DNA sequencing confirmed the identity of all PCR products. Sequencing service was performed by Research Biolabs Singapore.

2.5. Reverse transcription and Real-time PCR of Cat S, Cat L, CD74, CIITA and RT1-Dα

Real-time PCR was performed using the ABI 7500 Real Time PCR System (Applied Biosystems, CA, USA). All reagents were purchased from this company unless otherwise stated. Total RNA was reverse transcribed to cDNA using reagents from the cDNA archive kit (4322171). 10 μg of total RNA was used in a total reverse transcription reaction volume of 100 μl. The RT step was performed for 10 min at 25 °C and 2 h at 37 °C. In real-time PCR, 20× TaqMan gene expression assay mix of Cat S (Rn01534427_m1), Cat L (Rn00565793_m1), CD74 (Rn01491430_g1), CIITA (Rn01424723_g1) and RT1-Dα (Rn02346209_g1), as well as 20× 18s rRNA (4319413E) were used. For each real-time target, the reaction comprises of 3 μl cDNA, 0.5 μl 20× 18S rRNA, 0.5 μl 20× TaqMan gene expression assay, 1 μl nuclease-free water and 5 μl TaqMan Universal PCR master mix (4352042). Conditions for PCR were 2 min 50 °C, 10 min 95 °C and 40 cycles of 15 s 95 °C and 1 min 60 °C. The comparative threshold method was used to quantitate relative changes of target mRNA (User Bulletin #2, Applied Biosystems). Relative quantitation of target mRNA was expressed as fold change in gene expression to control (untreated). The data presented are representative for three independent experiments with the same trend. The graphs were made using OrignPro 7 (OriginLab, MA, USA).

2.6. Immunostaining and microscopy

The primary cells were grown in DMEM supplemented with 10% FBS on glass cover slips in 24-well culture plates prior to staining with antibodies against GFAP, SMAA, Desmin, RECA-1, ED-2, cathepsin S, RT1-B and CD74. At 60–70% confluence, the cells were washed once with sterile PBS and fixed with 4% paraformaldehyde (PFA) for 30 min at 4 °C, followed by three washes with PBS. The cells were blocked and permeabilized in blocking solution (10% horse serum, 0.1% Triton X-100 in PBS) for 1 h at 37 °C. The primary antibody was incubated in 10% blocking solution in PBS for 1 h at 37 °C followed by the secondary antibody under the same conditions. The primary antibody was omitted as a negative control. All images were taken with the LEICA DM IRB epifluorescence microscope using a 63× objective.

For induction experiments, IFN-γ was added to the cell culture at low confluence and the cells were cultivated further for different times depending on the targets to be stained (Cat S: 0, 4, 8, 24, 30 h; CD74: 0, 8, 24, 30 h; and RT1-B: 0, 24, 48 h). The presented images are representative for 3 experiments. Images were taken with a 40× objective. The fluorescence intensities from 3 to 7 different fields of vision of one representative experiment were quantified using the Image processing toolbox of the MATLAB platform (MathWorks, MA, USA).

The following antibodies were used in the immunofluorescent staining. Anti-Cat S antibody (sc-6505) and anti-CD74 antibody (sc-5438) were from Santa Cruz Biotechnology (CA, USA); anti-RT1-B antibody (554926) was from BD Pharmingen (CA, USA); anti-GFAP antibody (Z 0334) was from Dako (CA, USA); and anti-SMAA (smooth muscle alpha-actin)-Cy3 (C 6198) and anti-desmin antibody (D 8281) were from Sigma Chemicals (MO, USA). The anti-RECA-1 antibody (MCA970) and anti-ED-2 (CD163, MCA342R) were from Serotec (Oxford, UK). The secondary antibodies used were anti-goat-Alexa488 (A-21467, Invitrogen), anti-rabbit-FITC (F 0382, Sigma) and anti-mouse-FITC (F 0257, Sigma).

2.7. Cathepsin S activity measurement

The cells were grown in cell culture medium containing 10% FBS in 75 cm² flasks. When the cells reached 50–60% confluence, IFN-γ was added at 10 ng/ml or omitted as untreated sample. The cells were harvested 48 h later and resuspended in CS cell lysis buffer. Cathepsin S activity was measured using a kit from BioVision (K1101-01) according to the provided manual. The final substrate concentration was 200 μM. Emitted fluorescence was measured using the Tecan Safire II (Tecan, Zurich, Switzerland) fluorescence plate reader at λ_{ex}: 400 nm and λ_{em}: 505 nm. An AFC standard curve was used to calculate the released fluorophore in μM per μg protein per hour at 37 °C.

2.8. Antigen uptake and processing experiment

The cells were grown to 70% confluence and incubated with 100 μg/ml DQ-ovalbumin (Invitrogen) for 15 min at 37 °C or 4 °C (control) and then washed twice with medium. The cells were further incubated at 37 °C and mounted onto microscope slides after different time points. The uptake and digest of the tracer ovalbumin was imaged with the LEICA DM IRB epifluorescence microscope using the FITC filter. Representative images of 3 independent experiments were shown.

3. Results

3.1. HSC isolation and characterization

Primary HSCs were isolated from Wistar rat livers according to a previously published protocol [19], and seeded into 75 cm² culture flasks or onto glass cover slips. At the same time, part of the cell pellet was also used for total RNA isolation. To confirm the HSC identity, primary cells cultured for 3 days were stained with antibodies against GFAP, desmin, and SMAA respectively. As illustrated in Fig. 1, cells in short-term (3 days) culture displayed prominent filamentous GFAP staining (Fig. 1A) in numerous (but not all) cells, along with staining for two other HSC markers, desmin (Fig. 1B) and SMAA (Fig. 1C). In the subsequent 7 days, the cells gradually lost the strong filamentous GFAP staining (data not shown). At the same time, cells acquired very pronounced SMAA staining, with a typical filamentous distribution. Notably the intense SMAA staining even extended to the nucleus (Fig. 1D), suggesting that the HSCs are at a highly activated state. The purity of our HSC preparation was estimated to be greater than 95% according to GFAP positive staining (data not shown). In addition, the cells

were stained negative for RECA-1 antigen, a marker for endothelial cells. A small percentage of cells stained positive for ED-2 (CD163), a Kupffer cell marker, within the first few days (data not shown). In order to confirm that the activated HSCs used in our study were not contaminated by Kupffer cells we performed a RT-PCR using primers for a specific Kupffer cell marker (77- to 88-kDa fucose receptor). The RT-PCR could not detect this marker within 30 cycles (data not shown).
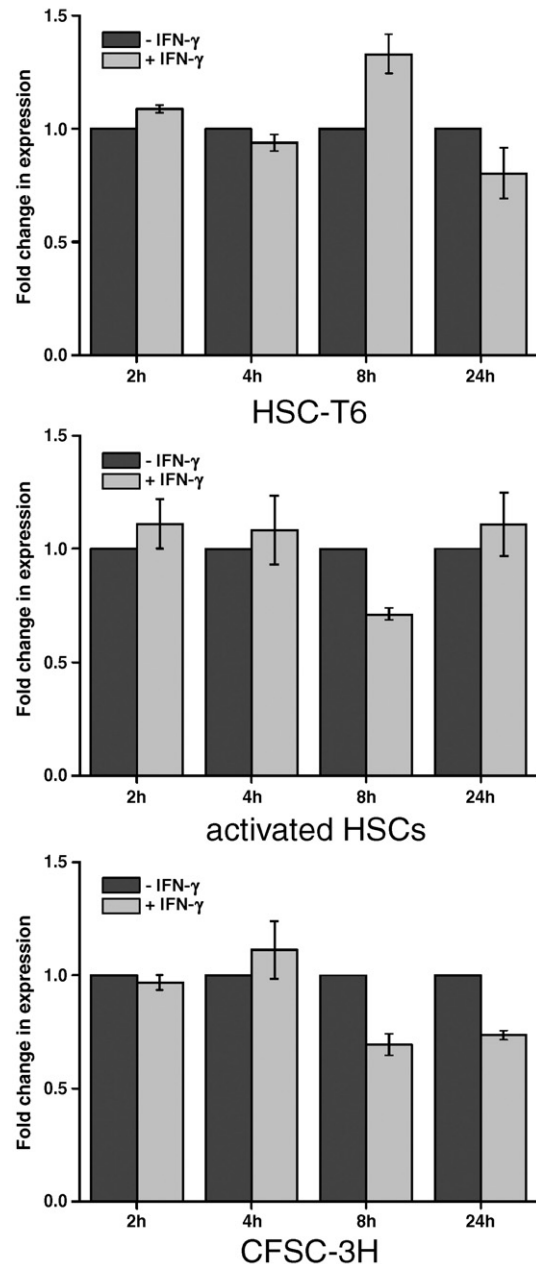

Fig. 4. Real-time RT-PCR analysis of the cathepsin L transcript level after IFN-γ treatment. The cells were treated with IFN-γ for 2, 4, 8 and 24 h, total RNA was extracted from activated HSCs, HSC-T6 and CFSC-3H respectively. After reverse transcription, the cathepsin L mRNA level was analyzed using real-time RT-PCR. Using the relative quantification method, the results were expressed as fold change in gene expression compared to the untreated samples. The graphs illustrate the lack of change in cathepsin L mRNA level after treatment with IFN-γ.

3.2. Transcriptional expression of early molecules required for antigen presentation in HSCs

In order to investigate whether HSCs express the main molecules required in the beginning of antigen presentation at the transcriptional level, specific RT-PCR primer pairs (Table 1) were designed. The molecules studied included the class II transactivator (CIITA), which is the major transcriptional regulator of MHC class II molecules, being a transcriptional co-activator; the MHC class II molecules (RT1-Dα and RT1-Bα) themselves; the invariant chain (CD74), a chaperone for the MHC class II molecules, and cathepsin S, which is a lysosomal protease predominantly expressed in antigen presenting cells and lymphatic tissues, and has been implicated in the processing of the invariant chain in certain cell types [16–18]. We included an established cell line derived from a CCl$_4$-induced fibrotic liver in our study in order to investigate whether a different history of activation makes a difference with respect to the expression of the studied molecules. Total RNA were isolated from primary HSCs that had been culture activated for 36 days, as well as from the HSC-T6 and CFSC-3H cell lines cultured in the absence of IFN-γ. As shown in Fig. 2, the activated HSCs and both cell lines had the same expression pattern for Cat S,

CD74, RT1-Bα and RT1-Dα and showed a basal transcript level of these molecules.

Interestingly, both type IV CIITA, (known as the major IFN-γ inducible transactivator [21]) and type III CIITA (known to regulate the constitutive class II expression in B-cells [22]) were expressed in activated HSCs, as well as in HSC-T6 (Fig. 2A and B), but not in CFSC-3H (Fig. 2C). Because we were unable to detect the CIITA types III and IV in the CFSC-3H cell line, we tested whether they are expressing the type I. Indeed we found the sole expression of type I in this cell line (Fig. 2D). In contrast, type I was not expressed in HSC-T6 and activated HSCs (data not shown). Noteworthy is also that the expression of cathepsin S [23] and CIITA type III [24] was shown for gliomas.

The mRNA for cathepsin L, another lysosomal cysteine protease, which could be involved in the CD74 processing, was present in all cells used (data not shown).

3.3. Quantitative analysis of IFN-γ effect on mRNA transcripts of Cat S, Cat L, CD74, CIITA and RT1-Dα

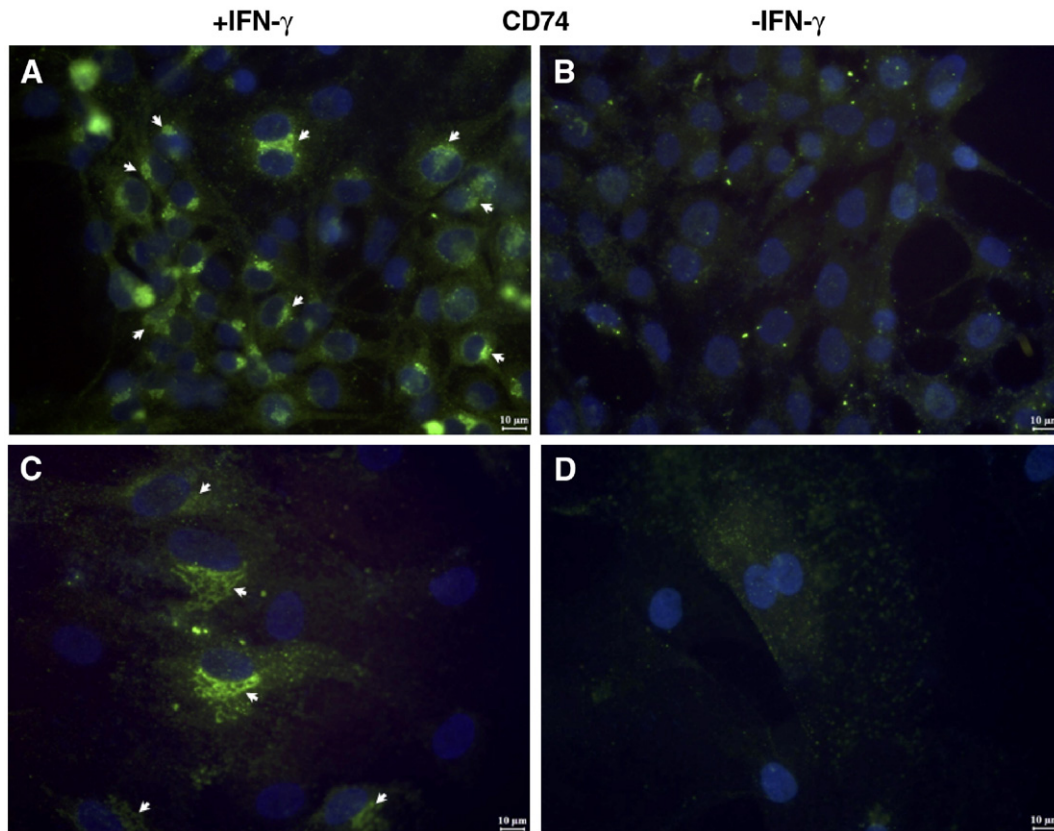Initial experiments, using OneStep RT-PCR, established that the above mentioned molecules were expressed in

Fig. 5. Effect of IFN-γ treatment on the expression of CD74 in HSC-T6 cells and activated HSCs. HSC-T6 and activated HSCs were plated and grown to a confluence of 60–70% overnight at conditions described in Materials and methods. The cells were treated with IFN-γ for a different period of time. Images (A) and (C) showed the immunofluorescence staining with anti-CD74 antibody after 30 h of IFN-γ induction for HSC-T6 and activated HSCs respectively (Arrows depict the increase in fluorescence). (B) and (D) displayed the controls without IFN-γ for HSC-T6 and activated HSCs respectively. Cells were counterstained with DAPI (blue). Scale bar=10 μm.

activated HSCs, HSC-T6 and CFSC-3H. We were interested in their response towards treatment with the proinflammatory cytokine IFN-γ. The transcripts for CIITA, CD74, RT1-Dα and Cat S were detected by quantitative real-time RT-PCR using Taqman assays (Fig. 3A–C) and are presented as fold change in gene expression relative to the untreated sample. Upon induction with IFN-γ, we observed that the CIITA (note that the Taqman assay detects all variants) and the cathepsin S transcripts in HSC-T6 (Fig. 3A), activated HSCs (Fig. 3B) and CFSC-3H (Fig. 3C) started to increase at an early time point, which was in general agreement with earlier observations [25,26]. While the increase in the CIITA transcript level was similar in HSC-T6 and CFSC-3H, it was more then 20 times higher in activated HSCs. Even though the cathepsin S transcription was upregulated by IFN-γ (somewhat slower for the HSC-T6), there is an order of magnitude difference in the change of the mRNA level in the following order HSC-T6<activated HSC<CFSC-3H.

As expected, the mRNA expression of the MHC class II molecule (RT1-Dα), and the invariant chain (CD74) were also induced, but indirectly through the subsequent action of CIITA at a later time. This type of activation by CIITA is reviewed in [27]. As can be seen from the graphs (Fig. 3A–C), the fold change in gene expression for CD74 and RT1-Dα compared to the control is much lower in HSC-T6 than in activated HSCs and CFSC-3H. The difference is about 10 to 20 times.

We knew from initial experiments that cathepsin L is expressed in activated HSCs, HSC-T6 and CFSC-3H. Because cathepsin L is used in the thymus for the processing of CD74, we wanted to see if the cathepsin L mRNA is upregulated in hepatic stellate cells. Contrary to the observation for cathepsin S, IFN-γ treatment had no influence on cathepsin L mRNA level. In fact, after 8 h, the cathepsin L mRNA expression decreased in CFSC-3H (Fig. 4).

3.4. Upregulation of CD74, RT1-B and cathepsin S proteins

In order to show that the increase in mRNA level also reflects an increase in protein expression, immunofluorescence staining was used to assess the respective proteins in both the untreated and IFN-γ treated cells at different time points. For these experiments, we used the HSC-T6 and the activated HSCs. Upregulation of CD74 expression under IFN-γ treatment was observed for HSC-T6 (Fig. 5A) and activated HSCs (Fig. 5C). CD74 expression was significantly induced by IFN-γ after 30 h, as shown by arrows in the micrographs,
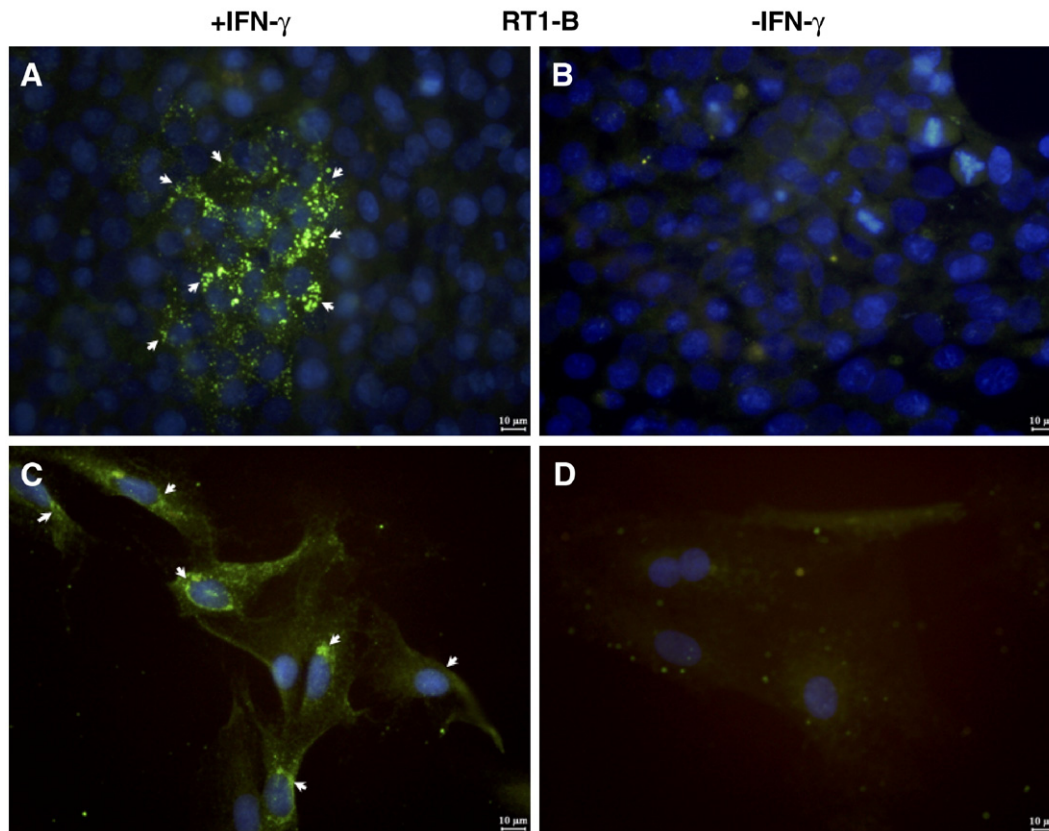

Fig. 6. IFN-γ effect on the expression of MHC class II molecule RT1-B in HSC-T6 and activated HSCs. HSC-T6 and activated HSCs were plated and grown to a confluence of 60–70% overnight at conditions described. The cells were treated with IFN-γ for 48 h and immunologically stained as described in Materials and methods. Images (A) and (C) showed the immunofluorescence of the anti-RT1-B antibody after 48 h of induction, for HSC-T6 and activated HSCs respectively (Arrows show the increase in immunofluorescence). In (B) and (D) are the respective controls without addition of IFN-γ. Cells were counterstained with DAPI (blue). Scale bar=10 μm.

and exhibited a typical perinuclear staining. This observation is consistent with the trafficking pattern of membrane-targeted proteins. On the contrary, HSCs under untreated conditions showed a much weaker or barely detectable staining of CD74 (Fig. 5B, D). Similarly, the expression of RT1-B in both the HSC-T6 cell line (Fig. 6A) and activated HSCs (Fig. 6C) was also induced after 48 h of IFN-γ treatment. Newly synthesized RT1-B proteins were visible in the perinuclear region (depicted by arrows). This observation is consistent with ER/Golgi localization. Interestingly the immunofluorescence staining for CD74 and RT1-B was never homogenously distributed over the cells, which leads us to the assumption of heterogeneity among the HSC population regarding their inducibility by IFN-γ.

We have shown earlier on that there was an increase in the cathepsin S mRNA in HSC-T6 and activated HSCs treated with IFN-γ (Fig. 3A, B). At first it seems that our immunofluorescent approach failed to convincingly document an induction in cathepsin S at the antigen level at 8 h respectively for HSC-T6 and activated HSCs (Fig. 7A, C). However, quantification of the fluorescence intensities from different areas of the same experiment showed that IFN-γ resulted also in a significant increase in cathepsin S expression on the protein level for HSC-T6 and the activated HSCs (Fig. 8).

3.5. Cathepsin S activity upon induction with IFN-γ

To further investigate the induction of cathepsin S by IFN-γ, activity measurement was performed to directly detect cathepsin S in activated HSCs and both cell lines. There was a significant increase of cathepsin S specific activity in HSC-T6, activated HSCs and CFSC-3H ($P < 0.05$) after 48 h (Fig. 9). This activity was almost completely inhibited by the cathepsin S inhibitor provided with the kit (data not shown).

3.6. Uptake and processing of ovalbumin

Successful antigen presentation requires the HSCs to internalize antigenic proteins and to process them into smaller peptides. To demonstrate these capabilities of activated HSCs and HSC-T6, a quenched tracer DQ-ovalbumin was used in the experiments. DQ-ovalbumin is strongly labeled with the fluorescent BODIPY FL dye, whereby the fluorescence is quenched in the intact ovalbumin protein. Upon digestion into peptides, the fluorescence is released and can be detected with a standard fluorescein optical filter. The uptake of ovalbumin was thought to occur through receptor-mediated endocytosis by the Mannose receptor [28,29]. In our case, the HSCs (activated HSCs as well as HSC-T6) took up the ovalbumin and processed
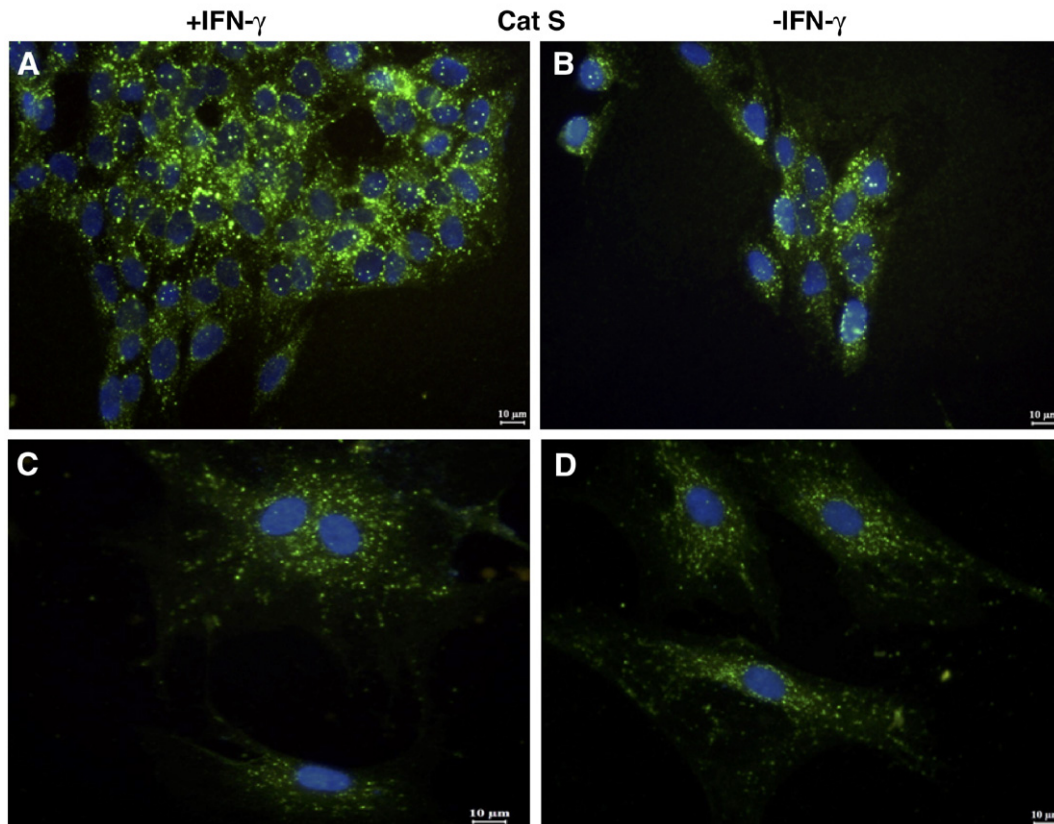

Fig. 7. Expression of cathepsin S in the IFN-γ treated and untreated HSC-T6 and activated HSCs. HSC-T6 and activated HSCs were plated and grown to a confluence of 60–70% overnight at conditions described. The cells were treated with IFN-γ for 8 h and stained by immunofluorescence as described in Materials and methods. Images (A) and (C) represented the immunofluorescence with anti-cathepsin S antibody after 8 h of incubation with IFN-γ for HSC-T6 and activated HSCs respectively. Images (B) and (D) are the corresponding controls for the HSC-T6 and activated HSCs. Cells were counterstained with DAPI (blue). Scale bar = 10 μm.
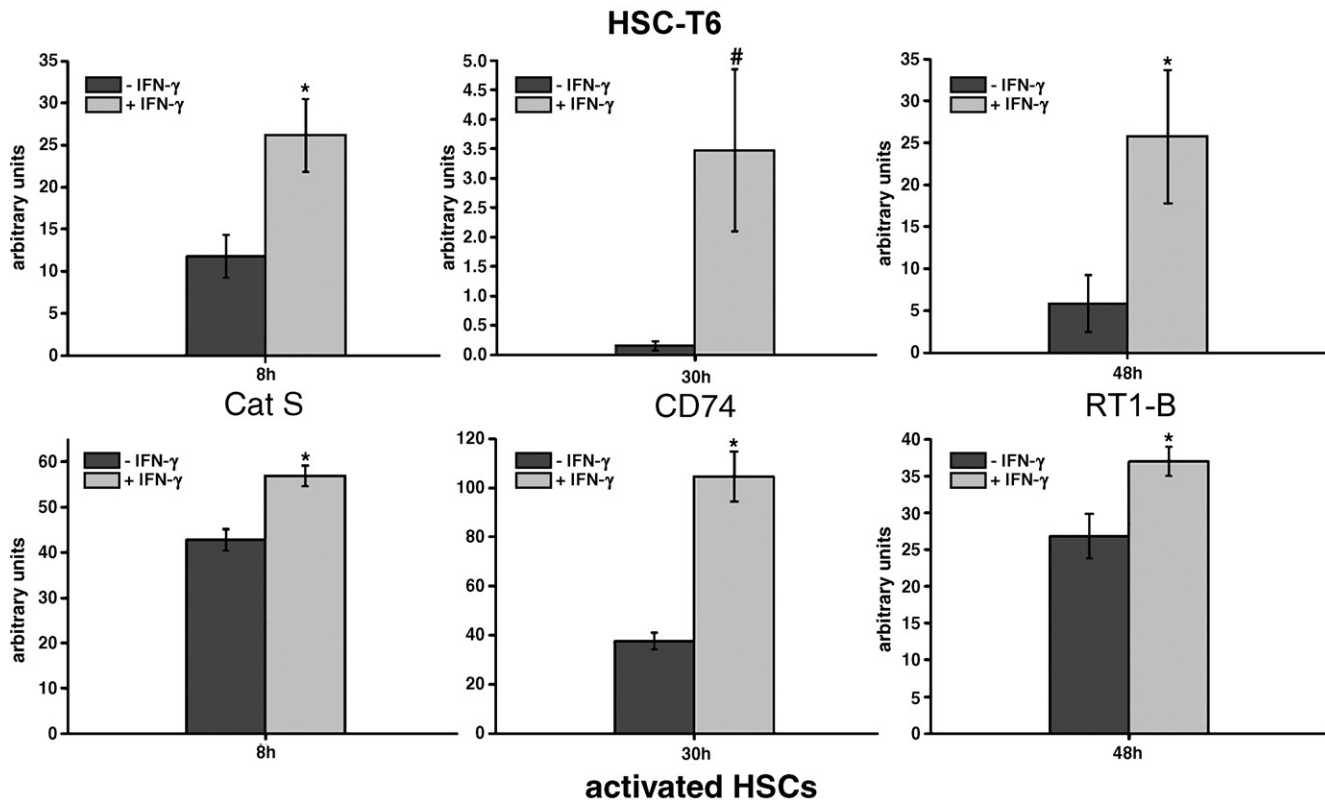
Fig. 8. Quantification of the fluorescence intensities. Several fields of vision were used to quantify the total fluorescence with a boundary to the nuclei. The values were normalized to the area. Data are presented as mean±SD *$P<0.05$, #$P<0.1$.

it within 15 min (data not shown). After an additional processing time of 30 min, a shift in the fluorescence emission from green to orange became apparent as shown in Fig. 10. This shift was due to the formation of so-called excimer at spots with highly localized and concentrated digested peptide tracer, as described in the manufacturer's instructions. The activated HSCs showed a

very strong green-yellow autofluorescence around the nucleus. As a result, the green dots were not detectable, but orange stained vesicles became discernable after 30 min of incubation. This shows not only the uptake but also the successful processing of the antigen.

4. Discussion

Recently published papers demonstrated by flow cytometric analysis that the MHC class II molecule (HLA-DR), and co-stimulatory molecules (such as CD40, CD80 and CD86) can be stimulated by IFN-γ in HSCs [4,5]. However, no information was available concerning the early events of antigen presentation and about the molecules involved in these events. Among them, CIITA type IV the transactivator of class II molecules is considered as a 'major regulator' for other molecules, like MHC class II molecules and invariant chain (CD74), and is responsive to IFN-γ [14,27]. Furthermore, the invariant chain was known to be involved in the assembly of the MHC class II molecules [30]. As the invariant chain is blocking the antigen-binding pocket of the class II molecule, it has to be degraded by proteases. Two of the proteases involved in the processing are cathepsin L and cathepsin S, which participate, depending on the cell type [15–18], in the latter steps of degradation of the invariant chain.

The aim of the current study was to obtain more detailed information on the molecular mechanisms underlying antigen
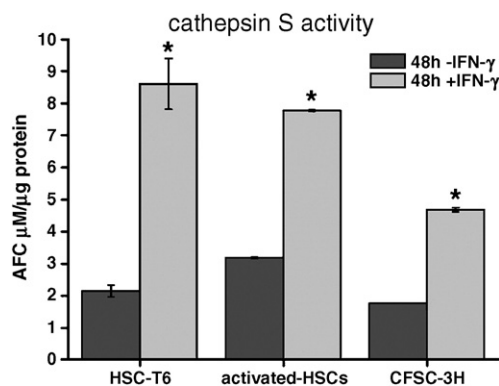

Fig. 9. Cathepsin S activity in activated HSCs and two different cell lines. The cells were grown in cell culture medium containing 10% FBS. When they reached 50–60% confluence, IFN-γ was added or omitted as control. The cells were harvested 48 h later and resuspended in CS cell lysis buffer. Cathepsin S activity was measured using a final substrate concentration of 200 μM. The specific activity is given in released fluorophore (AFC) in μM per μg protein per hour at 37 °C. Data are presented as mean±SD *$P<0.05$.
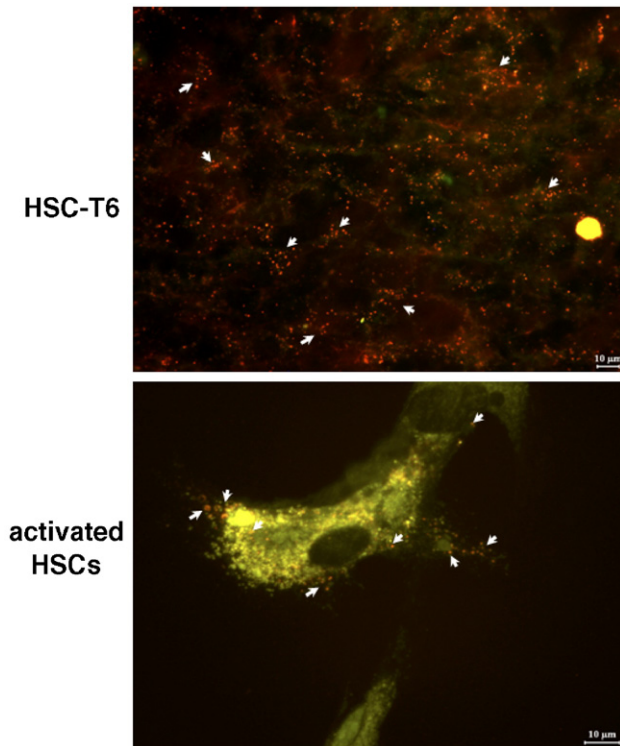
Fig. 10. Uptake and processing of labeled ovalbumin. The cells were initially incubated with DQ-ovalbumin for 15 min at 37 °C and then washed twice with medium. Subsequently the cells were incubated in medium alone for an additional 30 min, and imaged with a Leica epifluorescence microscope. The images showed the uptake and digest of the DQ-ovalbumin by HSC-T6 and activated HSCs respectively. Arrows referred to the red-shifted excimer formed by high concentrations of digested ovalbumin. Scale bar=10 μm.

presentation in HSCs. Here, quantitative RT-PCR and immunofluorescence methods were employed to study the molecules involved in the early stage of antigen presentation. Along with culture activated HSCs, we used in our study two cell lines. The HSC-T6 is a SV40 immortalized HSC cell line, regarded as semi-activated, whereas the CFSC-3H is derived from a cirrhotic liver and is regarded as *in vivo* activated. For the first time, we showed that activated HSCs, as well as the HSC cell lines HSC-T6 and CFSC-3H expressed transcripts for all molecules studied, namely CIITA, RT1-Bα, RT1-Dα, CD74, and cathepsin S (Fig. 2A–C). Interestingly we found that in addition to CIITA type IV (common to non-professional APCs), the CIITA type III was also expressed in HSCs. The transcript for CIITA type III was clearly detectable in activated HSCs and the HSC-T6 cell line, but not in CFSC-3H (Fig. 2A–C). This finding was particularly interesting as CIITA type III has been reported in another publication [31] to be induced by IFN-γ and subsequently mediated the repression of collagen (col1a2) in fibroblasts. We also discovered in the current study that the type III transcript in the HSCs was inducible by IFN-γ (data not shown). There could be some relationship between the expression of CIITA type III and the regulation of collagen expression in hepatic stellate cells. For the CFSC-3H we found solely the expression from the CIITA promoter type I (Fig. 2D). This type of CIITA

is expressed in dendritic cells and IFN-γ induced macrophages [14]. Whether this switch between the different CIITA promoters is a representation of the collagen production in fibrotic HSCs has to be studied. We did not pursue the question of the different expression of CIITA in this study, although this finding has potential in the perspective of the treatment of fibrotic HSCs.

Apparently CIITA, being the master regulator for the MHC class II expression, was responding as expected. The increase in mRNA level started early after addition of IFN-γ (Fig. 3A–C). The CIITA mediates the IFN-γ effect as shown by Steimle et al. [21] and induced the increase in the mRNA levels of the MHC class II molecules and the invariant chain (CD74) as visualized at the later time-points (Fig. 3A–C). The immunofluorescence data for the CD74 and RT1-B molecules (Figs. 5 and 6) were in accordance with the quantitative RT-PCR data. The invariant chain was detectable after 24 h, but the difference in its expression between treated sample and control was best seen after 30 h (Fig. 5A, C). RT1-B expression however, was best detectable after 48 h (Fig. 6A, C). We quantified the fluorescence images and found a significant difference in the fluorescence intensities when comparing IFN-γ treated and untreated samples (Fig. 8).

The best studied function of cathepsin S is the processing of the invariant chain by releasing the CLIP from lip10 [18]. Therefore the finding that cathepsin S is expressed in HSCs and can be upregulated with the proinflammatory cytokine IFN-γ (Figs. 3A–C and 7) seems to suggest a possible contribution to the CD74 processing. This is substantiated by the increase in cathepsin S activity compared to the control (Fig. 9). On the other hand, cathepsin L which is another possible candidate for the final processing of the invariant chain [15], showed no significant increase on the transcription level (Fig. 4). These results present the first indication towards a role of cathepsin S in HSCs. In order to conclude the involvement of cathepsin S in the processing of the invariant chain in HSCs, further studies are required.

While we investigated the response of CIITA, CD74, RT1-Dα and cathepsin S to IFN-γ using quantitative real-time PCR, we made another remarkable finding. Although the expression of these molecules increased after induction with IFN-γ, there were differences in the degree of their upregulation for the different HSCs (Fig. 3A–C). This phenomenon could be explained by the different basal expression of these molecules. The differences in origin of these cells, (cell culture activated HSCs, SV40 immortalization HSC-T6 and derivation from cirrhotic liver CFSC-3H) could also have an influence on the expression level. The stability of the transcripts could be differentially regulated in the various HSCs studied.

Finally we showed that the hepatic stellate cells were capable of taking up antigenic proteins such as ovalbumin. More importantly, HSCs also own the molecular machinery needed to process them into smaller peptides (Fig. 10). The efficiency of this process was comparable in HSC-T6 and activated HSCs.

In conclusion, we have shown that activated hepatic stellate cells feature all molecules necessary for the early stage of

antigen presentation. Furthermore, the HSCs are able to upregulate these molecules in response to IFN-γ, independent of their origin of activation. There was however a difference in the degree of upregulation. Another significant finding is that cathepsin S, a lysosomal cysteine protease primarily involved in the processing of CD74, was found in HSCs. This is important because this enzyme is a main target in treating autoimmune diseases [32] and seems to be involved in angiogenic processes [33,34]. In order to define the intrinsic role of cathepsin S in HSCs, more investigations have to be done. But it became clear from this study that the lysosomal protein degradation is not the only function of cathepsin S. The finding that different CIITA promoters are used in HSC-T6, activated HSCs and the fibrotic CFSC-3H could point to another therapeutic target specific for fibrotic HSCs. We have also compared the HSC-T6 cell line with culture activated HSCs and concluded that this cell line retained many of the key features of the activated cells regarding antigen presentation. This cell line is thus suited for studying the molecular events that occurred during antigen presentation in HSCs.

Acknowledgements

References

[1] M. Sato, S. Suzuki, H. Senoo, Hepatic stellate cells: unique characteristics in cell biology and phenotype, Cell Struct. Funct. 28 (2003) 105–112.

[2] R. Bataller, D.A. Brenner, Hepatic stellate cells as a target for the treatment of liver fibrosis, Semin. Liver Dis. 21 (2001) 437–451.

[3] S. Lotersztajn, B. Julien, F. Teixeira-Clerc, P. Grenard, A. Mallat, Hepatic fibrosis: molecular mechanisms and drug targets, Annu. Rev. Pharmacol. Toxicol. 45 (2005) 605–628.

[4] O. Viñas, R. Bataller, P. Sancho-Bru, P. Ginès, C. Berenguer, C. Enrich, J.M. Nicolás, G. Ercilla, T. Gallart, J. Vives, V. Arroyo, J. Rodés, Human hepatic stellate cells show features of antigen-presenting cells and stimulate lymphocyte proliferation, Hepatology 38 (2003) 919–929.

[5] M.C. Yu, C.H. Chen, X. Liang, L. Wang, C.R. Gandhi, J.J. Fung, L. Lu, S. Qian, Inhibition of T-cell responses by hepatic stellate cells via B7-H1-mediated T-cell apoptosis in mice, Hepatology 40 (2004) 1312–1321.

[6] C. Gabay, I. Kushner, Acute-phase proteins and other systemic responses to inflammation, N. Engl. J. Med. 340 (1999) 448–454.

[7] S.J. Wigmore, K.C. Fearon, J.P. Maingay, P.B. Lai, J.A. Ross, Interleukin-8 can mediate acute-phase protein production by isolated human hepatocytes, Am. J. Physiol. 273 (1997) E720–E726.

[8] A. Limmer, J. Ohl, C. Kurts, H.G. Ljunggren, Y. Reiss, M. Groettrup, F. Momburg, B. Arnold, P.A. Knolle, Efficient presentation of exogenous antigen by liver endothelial cells to CD8+ T cells results in antigen-specific T-cell tolerance, Nat. Med. 6 (2000) 1348–1354.

[9] Y. Shiratori, K. Okano, K. Matsumoto, S. Murao, Antigen presentation by Kupffer cells in the rat, Scand. J. Gastroenterol. 19 (1984) 733–739.

[10] C.R. Roland, L. Walp, R.M. Stack, M.W. Flye, Outcome of Kupffer cell antigen presentation to a cloned murine Th1 lymphocyte depends on the inducibility of nitric oxide synthase by IFN-gamma, J. Immunol. 153 (1994) 5453–5464.

[11] P.J. O'Connell, A.E. Morelli, A.J. Logar, A.W. Thomson, Phenotypic and functional characterization of mouse hepatic CD8 alpha+ lymphoid-related dendritic cells, J. Immunol. 165 (2000) 795–803.

[12] C. Johansson, M.J. Wick, Liver dendritic cells present bacterial antigens and produce cytokines upon Salmonella encounter, J. Immunol. 172 (2004) 2496–2503.

[13] A.H. Lau, A.W. Thomson, Dendritic cells and immune regulation in the liver, Gut 52 (2003) 307–314.

[14] S. LeibundGut-Landmann, J.M. Waldburger, M. Krawczyk, L.A. Otten, T. Suter, A. Fontana, H. Acha-Orbea, W. Reith, Mini-review: specificity and expression of CIITA, the master regulator of MHC class II genes, Eur. J. Immunol. 34 (2004) 1513–1525.

[15] T. Nakagawa, W. Roth, P. Wong, A. Nelson, A. Farr, J. Deussing, J.A. Villadangos, H. Ploegh, C. Peters, A.Y. Rudensky, Cathepsin L: critical role in Ii degradation and CD4 T cell selection in the thymus, Science 280 (1998) 450–453.

[16] R.J. Riese, R.N. Mitchell, J.A. Villadangos, G.P. Shi, J.T. Palmer, E.R. Karp, G.T. De Sanctis, H.L. Ploegh, H.A. Chapman, Cathepsin S activity regulates antigen presentation and immunity, J. Clin. Invest. 101 (1998) 2351–2363.

[17] C. Beers, A. Burich, M.J. Kleijmeer, J.M. Griffith, P. Wong, A.Y. Rudensky, Cathepsin S controls MHC class II-mediated antigen presentation by epithelial cells in vivo, J. Immunol. 174 (2005) 1205–1212.

[18] C. Driessen, R.A. Bryant, A.M. Lennon-Dumenil, J.A. Villadangos, P.W. Bryant, G.P. Shi, H.A. Chapman, H.L. Ploegh, Cathepsin S controls the trafficking and maturation of MHC class II molecules in dendritic cells, J. Cell Biol. 147 (1999) 775–790.

[19] L. Riccalton-Banks, R. Bhandari, J. Fry, K.M. Shakesheff, A simple method for the simultaneous isolation of stellate cells and hepatocytes from rat liver tissue, Mol. Cell. Biochem. 248 (2003) 97–102.

[20] S. Vogel, R. Piantedosi, J. Frank, A. Lalazar, D.C. Rockey, S.L. Friedman, W.S. Blaner, An immortalized rat liver stellate cell line (HSC-T6): a new cell model for the study of retinoid metabolism in vitro, J. Lipid Res. 41 (2000) 882–893.

[21] V. Steimle, C.A. Siegrist, A. Mottet, B. Lisowska-Grospierre, B. Mach, Regulation of MHC class II expression by interferon-gamma mediated by the transactivator gene CIITA, Science 265 (1994) 106–109.

[22] A.M. Lennon, C. Ottone, G. Rigaud, L.L. Deaven, J. Longmire, M. Fellous, R. Bono, C. Alcaide-Loridan, Isolation of a B-cell-specific promoter for the human class II transactivator, Immunogenetics 45 (1997) 266–273.

[23] T. Flannery, D. Gibson, M. Mirakhur, S. McQuaid, C. Greenan, A. Trimble, B. Walker, D. McCormick, P.G. Johnston, The clinical significance of cathepsin S expression in human astrocytomas, Am. J. Pathol. 163 (2003) 175–182.

[24] J.M. Soos, J.I. Krieger, O. Stuve, C.L. King, J.C. Patarroyo, K. Aldape, K. Wosik, A.J. Slavin, P.A. Nelson, J.P. Antel, S.S. Zamvil, Malignant glioma cells use MHC class II transactivator (CIITA) promoters III and IV to direct IFN-gamma-inducible CIITA expression and can function as nonprofessional antigen presenting cells in endocytic processing and CD4(+) T-cell activation, Glia 36 (2001) 391–405.

[25] K. Storm van's Gravesande, M.D. Layne, Q. Ye, L. Le, R.M. Baron, M.A. Perrella, L. Santambrogio, E.S. Silverman, R.J. Riese, IFN regulatory factor-1 regulates IFN-gamma-dependent cathepsin S expression, J. Immunol. 168 (2002) 4488–4494.

[26] M.A. Rahat, I. Chernichovski, N. Lahat, Increased binding of IFN regulating factor 1 mediates the synergistic induction of CIITA by IFN-γ and tumor necrosis factor-α in human thyroid carcinoma cells, Int. Immunol. 13 (2001) 1423–1432.

[27] J.A. Harton, J.P. Ting, Class II transactivator: mastering the art of major histocompatibility complex expression, Mol. Cell. Biol. 20 (2000) 6185–6194.

[28] G.M. Kindberg, S. Magnusson, T. Berg, B. Smedsrod, Receptor-mediated endocytosis of ovalbumin by two carbohydrate-specific receptors in rat liver cells. The intracellular transport of ovalbumin to lysosomes is faster in liver endothelial cells than in parenchymal cells, Biochem. J. 270 (1990) 197–203.

[29] S.A. Mousavi, M. Sato, M. Sporstol, B. Smedsrod, T. Berg, N. Kojima, H. Senoo, Uptake of denatured collagen into hepatic stellate cells: evidence for the involvement of urokinase plasminogen activator receptor-associated protein/Endo180, Biochem. J. 387 (2005) 39–46.

[30] J.A. Villadangos, Presentation of antigens by MHC class II molecules: getting the most out of them, Mol. Immunol. 38 (2001) 329–346.

[31] Y. Xu, L. Wang, G. Buttice, P.K. Sengupta, B.D. Smith, Major histocompatibility class II transactivator (CIITA) mediates repression of collagen (COL1A2) transcription by interferon gamma (IFN-gamma), J. Biol. Chem. 279 (2004) 41319–41332.

[32] H. Yang, M. Kala, B.G. Scott, E. Goluszko, H.A. Chapman, P. Christadoss, Cathepsin S is required for murine autoimmune myasthenia gravis pathogenesis, J. Immunol. 174 (2005) 1729–1737.

[33] G.P. Shi, G.K. Sukhova, M. Kuzuya, Q. Ye, J. Du, Y. Zhang, J.H. Pan, M. L. Lu, X.W. Cheng, A. Iguchi, S. Perrey, A.M.E. Lee, H.A. Chapman, P. Libby, Deficiency of the cysteine protease cathepsin S impairs microvessel growth, Circ. Res. 92 (2003) 493–500.

[34] B. Wang, J. Sun, S. Kitamoto, M. Yang, A. Grubb, H.A. Chapman, R. Kalluri, G.P. Shi, Cathepsin S controls angiogenesis and tumor growth via matrix-derived angiogenic factors, J. Biol. Chem. 281 (2006) 6020–6029.